Asociación Argentina
de Mecánica Computacional

Mecánica Computacional Vol XXXIV, págs. 313-330 (artículo completo)
Sebastián Giusti, Martín Pucheta y Mario Storti (Eds.)
Córdoba, 8-11 Noviembre 2016

CONFINED INFLATABLE STRUCTURES: FROM EXPERIMENTS TO SIMULATIONS

Eduardo M. Sosa[a], Jerry Choo-Sian Wong[a], and Ever J. Barbero[a]

[a] *Department of Mechanical and Aerospace Engineering, West Virginia University, 395 Evansdale Dr., Morgantown, West Virginia, USA, eduardo.sosa@mail.wvu.edu, http://statler.wvu.edu*

Keywords: Conformity, Deployment, Folding, Inflatable Structures, Modeling, Tunnel.

Abstract. The implementation of large-scale inflatable structures is now a viable alternative for sealing of segments of transportation tunnel in emergency situations. The rapid deployment of one or more inflatables can prevent the propagation of flooding, noxious gasses or smoke until more permanent containment and repair measures can be put into place. In such applications, the inflatable structure is prepared for placement, either permanently or temporary, and left ready for deployment, inflation, and pressurization when needed. The level of sealing effectiveness depends on the ability of the inflatable structure to deploy and self-accommodate, without human intervention, to the intricacies of the perimeter of the conduit being sealed. Once deployed, inflated and pressurized, the inflatable has to remain stable during the containment of the threat. Extensive testing at multiple scales was completed in the past years to evaluate and fine tune the functionality of the inflatable structure and associated subsystems. However, testing multiple scenarios and different configurations of the system can be very expensive and time-consuming, and, therefore, the development and calibration of finite element simulations of the system become imperative to predict possible outcomes and therefore, minimize the need for physical testing. This work presents an overview of the development of finite element simulations of the deployment and inflation of a full-scale inflatable prototype placed within a tunnel section. Techniques developed experimentally served as the basis for the development of computational models that can simulate different stages of folding, placement, initial deployment and full inflation. The good level of correlation between experimental and simulation results in terms of deployment dynamics and levels of contact demonstrated that the proposed modeling strategy could be used as a predicting tool for other tunnel shapes and sealing configurations.

1 INTRODUCTION

Alternative solutions have been proposed to seal segments of transportation tunnels prone to damage due to extreme events. The implementation of large-scale inflatable structures (also called inflatable plugs) inside transportation tunnels is intended to prevent or reduce the damage induced by hazardous events by creating a compartment to contain the propagation of a threat. Potential threats include flooding produced by heavy rains originated by hurricanes, smoke or noxious gasses originated by crashes or explosions. Any of these threats can propagate through the tunnel system and compromise its functionality and structural integrity (Lindstrand, 2010; Martinez et al. 2012).

In the recent years, West Virginia University (WVU) has conducted extensive testing for the development of high-pressure confined inflatable structures that can be placed at different locations along a tunnel and then rapidly deployed and pressurized to stop a tunnel flooding. The development of this solution progressed in stages from a proof-of-concept, air-inflated prototypes (Barrie, 2008; Martinez et al. 2012), to reduced and full-scale prototypes pressurized with water and subjected to back pressure for flooding simulations (Fountain, 2012; Barbero et al. 2013a; Sosa et al. 2014a, c). The sealing system is designed to be remotely activated when a threatening event is detected, which triggers the deployment and inflation of one or more of the inflatables to isolate and seal the tunnel segment under threat. The inflatable plugs are designed and prepared to have the ability to conform to the tunnel geometry and provide a tight seal to remain stable while containing the pressure of water or gasses (Barbero et al. 2013b; Sosa et al. 2014c).

Different testing efforts at different scales were reported to demonstrate the feasibility of containing flooding with inflatable structures, e.g. see Martinez et al. 2012, Barbero et al. 2013a and Sosa et al. 2014a, c. Under these efforts, multiple tests were performed in a specially built testing facility designed to simulate flooding of a tunnel segment. These tests generated valuable experimental information and provided several lessons for operation and field implementation. However, carrying out this type of tests, especially at the full-scale level, demonstrated to be a complex task in which only a select number of evaluations with a reduced number of iterations can be completed within the limits of the allocated time and resources.

The experimental work showed that the implementation of large-scale inflatable structures for sealing tunnel segments can be divided into three main phases: Phase 1, preparation and installation of the inflatable; Phase 2, initial deployment and inflation; and, Phase 3. Pressurization to contain flooding pressure or gas pressure.

In Phase 1, a folding pattern in conjunction with a packing procedure of the folded plug in a storage container are defined and implemented. Phase 2 starts when a threatening event is detected. The detection triggers the automatic opening of the storage container allowing the initial deployment of the inflatable. The initial deployment is followed by a low-pressure air inflation until the inflatable reaches its final shape and position for sealing specific tunnel segments. When the plug is fully inflated and completely positioned, Phase 3 starts with the pressurization process to maintain the inflatable stable, predominantly by friction, while it withstands the external pressure originated by flooding or gasses (Martinez et al. 2012; Barbero et al. 2013a; Sosa et al. 2014a-c).

Moreover, experiments carried out at full scale demonstrated that the sealing capacity of the pressurized inflatable is a function of the level of local and global conformity achieved during Phase 2. Full-scale tests of Phases 1 and 2 demonstrated that several iterations are necessary to achieve satisfactory levels of local conformity that cannot be predicted in advance. Therefore, the development of simulation models based on finite element (FE)

analysis contributes to predict the performance of the inflatable during the different phases outlined above.

This work provides an overview of the development of FE models created to reproduce different aspects of Phases 1 and 2 outlined previously. An overview of full-scale experimental work that served as a reference for the development of FE models is summarized first. Then, an overview of the modeling approach and a description of relevant components of the FE models are introduced. Simulation results and comparison with experimental results are presented next, and finally, a summary of main observations and conclusions are presented at the end.

2 OVERVIEW OF EXPERIMENTAL WORK

2.1 Inflatable structure and test preparation

The experimental work required the design and manufacturing of a full-scale inflatable structure used that was used as a testing prototype. The design followed the procedure outlined by Barbero et al. (2012b) and Sosa et al. (2014c). The inflatable consists of a cylindrical segment with two hemispherical end caps. The cylindrical segment is 4.940 meters in diameter and has a length of 4.641 meters. The radius of each hemispherical end cap is 2.469 meters, and the total length of the inflatable is 9.581 meters. The membrane of the inflatable consists of a three-layer system comprised of an internal bladder, an intermediate fabric restraint, and an external webbing restraint. The bladder is the innermost layer of the construction. It is in direct contact with the fluid used for inflation and pressurization. The intermediate fabric restraint protects the internal bladder. The external webbing restraint is a macro-fabric comprised of woven webbings designed to undertake all the membrane stresses generated by the pressurization. The macro-fabric of the outer layer consists of a plain weave pattern of 0.05 m wide webbings manufactured with Vectran fibers (Kuraray, 2012). From the structural point of view, the outer layer is the most important since it carries all the membrane stresses while the two inner layers provide air and water tightness required during the initial inflation and pressurization. All three layers contribute to the mass and volume of the inflatable. The inflation is carried out through aluminum fittings that are integrated into the membrane and function as either inflation or air release ports. The total weight of the inflatable plug is approximately 900 kg.

From the functionality point of view, the two most important geometric characteristics of the inflatable structure are:

1) The length of the cylindrical portion, considering that the inflatable is designed to remain stable by friction, the contact length was determined based on friction tests at coupon level and small-scale prototypes subjected to induced slippage over concrete surfaces typically found in segments of transportation tunnels (Sosa et al. 2014b). The length of the cylindrical portion of the plug provides sufficient contact length for the development of frictional forces to maintain the axial stability (Barbero et al. 2012b; Sosa et al. 2014c).

2) The perimeter of the cylindrical portion of the inflatable was designed to cover elements that typically exist in a tunnel cross-section. These elements include duct-banks, pipes, cables, and rails. The perimeter also includes a percentage of extra membrane material (typically in the range of 5-10%) to assure maximum local conformity of the inflatable to the tunnel surface.

The inflatable required preparation work before the execution of a test. A sequence of preparation steps was developed for folding and packing the deflated structure inside a portable container that was later placed inside a mockup tunnel section specially built for the

tests (Barbero et al. 2013a; Sosa et al. 2014a). These steps were developed to systematize the preparation process for multiple repetitions.

The sequence of preparation steps included: 1) Unconstrained inflation, surface inspection followed by a controlled deflation (in Figure 1, steps 1-2). 2) Attachment of the deflated inflatable to a portable container and attachment of tie-downs on the partially folded membrane (steps 3-4). The purpose of installing these tie-downs is to produce a sequential release of membrane material during the inflation to improve the level of local conformity on the lateral walls and corners as well as on the ceiling of the tunnel. 3) Folding by flat rolling (steps 5-6); 4) Packing of folded into the container and closing of the portable container (steps 6-7); and, 5) Transportation and securing the container into the tunnel mockup (step 8). The final position of the container on the sidewall of the tunnel mockup at the end of the preparation activities is illustrated in Figure 2(a). The initial inflation was carried out by a low-pressure inflation system connected to the inflatable as schematically shown in Figure 2(b).

Figure 1: Sequence of folding and packing implemented experimentally (Barbero et al. 2013a; Sosa et al. 2014a).

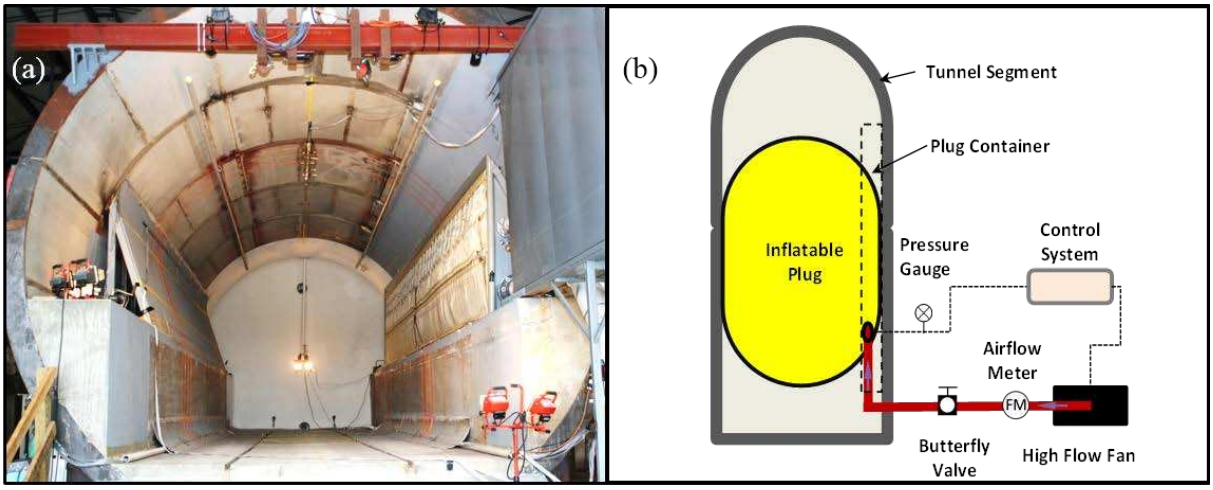

Figure 2: (a) Mockup of tunnel section with folded and packed inflatable installed on the right sidewall; (b) Schematic of low-pressure air inflation system connected to the inflatable (Barbero et al. 2013a; Sosa et al. 2014a).

2.2 Initial deployment and low-pressure air inflation

The deployment of the inflatable started with automatic activation of the opening mechanism installed on the container cover. The release of the cover allowed the folded plug to unroll by its own weight as the air inflation began. The air inflation process consisted of two parts: 1) The initial inflation was carried out with an airflow rate of 42 m^3/min until the plug pressure reached 1.7 kPa; then, 2) when the inflatable was fully positioned in the tunnel, the air flow was reduced to 1.4 m^3/min, and the plug pressure maintained constant around 2 kPa while the evaluations of global and local conformity took place. The total time from initial deployment to complete positioning in the tunnel was 180 seconds.

Low-pressure air inflation tests demonstrated that a key aspect for successful positioning of the inflatable was the sequential release of membrane material. The sequential release of the membrane was achieved by the tie-downs attached to the membrane installed during the folding process (see Figure 1, step 4). These tie-downs gradually broke and released membrane material in the last stage of the inflation and assured uniform coverage of the lateral corners located in the upper portion of the tunnel perimeter. Figure 3 illustrates the sequence of initial unrolling and subsequent low-pressure air inflation (Barbero et al. 2013a; Sosa et al. 2014a).

Figure 3: Sequence of initial unrolling and inflation captured during full-scale tests (Barbero et al. 2013a; Sosa et al. 2014a).

The folding and packing sequences outlined in Section 2.1 along with the dynamics of initial unrolling and inflation outlined in this section provided guidelines and reference points for the creation and development of the FE simulation models presented next.

3 OVERVIEW OF FE SIMULATION MODELS

3.1 Geometries and modeling approach

The development of a comprehensive model able to reproduce the different stages of the work performed experimentally required the creation of several components that constituted the whole FE model. The features of the different components of the FE model were defined considering the different phases outlined in previous sections. Specifically, The FE models presented in this section concentrated on reproducing Phase 1, which included folding, placement in the storage area, and Phase 2, which included initial deployment and inflation.

The two main components of the FE model are the inflatable structure and the tunnel segment in which the inflatable will be deployed. Additional components created in the modeling process included an auxiliary surface representative of the floor where the inflatable was placed before folding, as well as additional auxiliary plates that were created to replicate the folding procedures implemented in the full-scale prototype. The FE models of the inflatable, tunnel and auxiliary planes were created using Abaqus. Geometries, meshing, material properties and boundary conditions were created with Abaqus/CAE. Abaqus/Explicit

was used to solve the different portions of the FE models. Abaqus/CAE/Viewer was used to visualize results and generate graphical results obtained from the FE simulations (Abaqus, 2011).

The FE model of the inflatable plug was created assuming an unconfined, unstressed inflated condition with the nominal dimensions of the experimental prototype. Each hemispherical end cap included several partitions on its surface created for manufacturing purposes as well as for defining the inflation fittings as illustrated in Figure 4(a). Similarly, the cylindrical portion of the inflatable contained several partitions created to define folding lines and folding segments. Also, as in the experimental prototype, the perimeter of the cylindrical portion of the inflatable was oversized with respect of the tunnel perimeter. A 5% oversizing was added to achieve conformance of the plug to the tunnel and to take into account wrinkles and sag that may appear during the initial deployment and inflation.

As indicated in Section 2.1, the actual structural membrane of the inflatable consisted of a three-layer system. However, considering that only the outer layer contributes to the membrane strength and the inner layers contribute to the mass and volume of the inflatable, the multi-layer system was modeled with a single equivalent membrane with the same thickness as that the three-layer system. The three layers also contributed to the mass of the system, and only the outer layer (the macro-fabric of woven webbings) contributed the stiffness of the equivalent membrane. The FE model of the inflatable also included two aluminum fittings integrated into the membrane that function as air fill and air release ports. These two fitting are located on one of the hemispherical end caps. Considering that the fittings are much more rigid than the equivalent membrane, they were modeled with rigid elements (R3D4). As in the actual prototype, the total mass of the model of the inflatable including metallic fittings was 900 kg. Figure 4(b) shows the inflatable after meshing. The mesh consisted of nearly 31,000 triangular membrane elements with linear interpolation (M3D3).

The second main component of the FE model is the tunnel segment. In this study, the tunnel segment was assumed to be non-deformable. As such, quadrilateral rigid elements (R3D4) were used to represent the tunnel segment. The experimental tunnel profile is shown in Figure 2(a) was used as a reference for creating the FE model of the tunnel segment. Figure 4(c) shows a 3D rendering of the meshed configuration of the tunnel used in all the analyses. The tunnel section is also assumed to be fixed in X, Y, and Z directions. Similarly to the FE model of the tunnel segment, all the auxiliary plates created to simulate the folding process were considered non-deformable and meshed with R3D4 rigid elements.

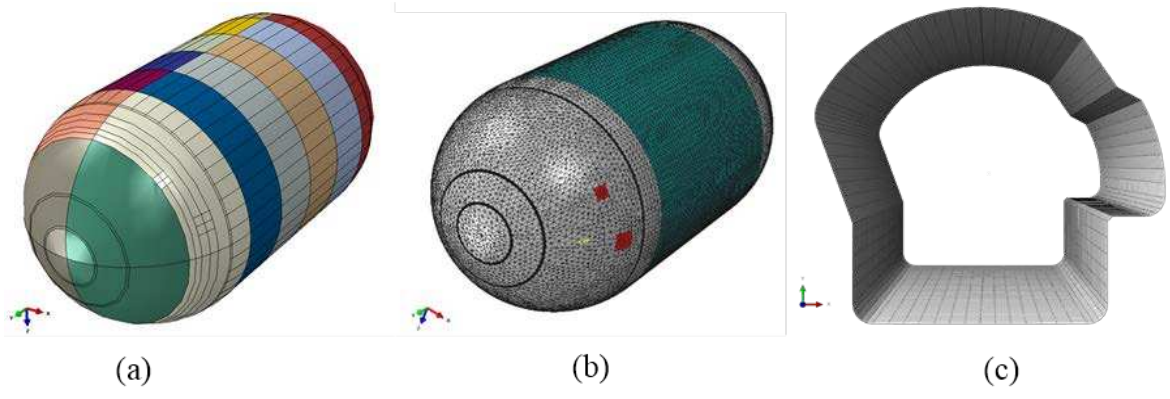

Figure 4: (a) Geometry and partitions of the inflatable; (b) FE mesh of the inflatable in unconfined conditions; (c) FE mesh of tunnel segment.

3.2 Simulation of folding

The folding sequence illustrated in Figure 1 guided the creation of the FE model of the folding process. As in the experimental work, the FE simulation of the folding process comprised the following stages: 1) Unconstrained, unstressed inflation; 2) flattening and grounding; 3) folding by successive flat rolling.

In the first stage, the inflatable has its nominal design geometry; it is also unstressed and in unconfined conditions. In the second stage, flattening is achieved by simultaneous application of horizontal displacements along two lines located in the cylindrical portion of the inflatable in conjunction with the action of a vertical gravity force. The two initial stages are illustrated in Figure 5, steps a-d.

Once the inflatable is flattened and laying on the ground (represented by the underlying grid in Figure 5), the folding process began by forming a longitudinal fold designed for temporarily holding and sequentially release of part of the membrane material during the inflation process as illustrated in Figure 5, steps e-h. Tie-downs held the membrane material contained in the first fold delimited by lines marked on the surface of the cylindrical portion of the inflatable. The tie-downs were modeled by connectors elements (CONN3D2) linking nodes placed along one of the longitudinal edges of the initial fold and nodes located at the underlying adjacent membrane as illustrated in Figure 1 (step 4), and in Figure 5 (step h). The connector elements were assigned to have only uniaxial strength and only a translational degree of freedom.

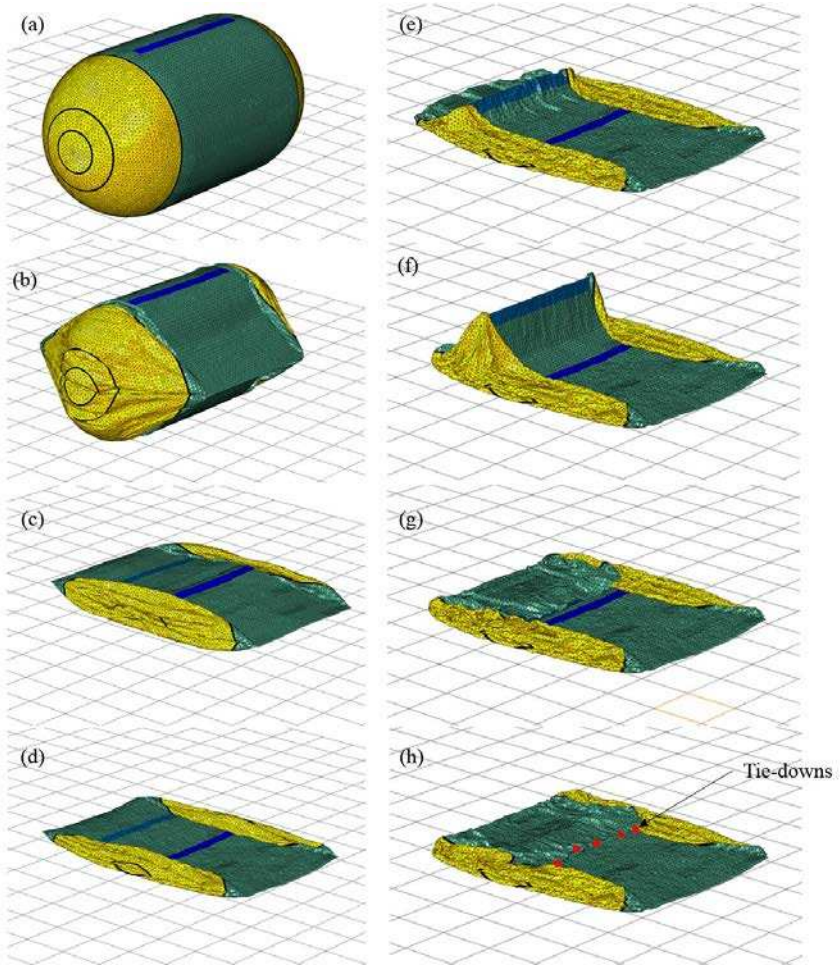

Figure 5: Simulation of folding (Part 1). Initial configuration and flattening (a-d); first fold for holding of membrane material (e-h).

In the third stage, the folding continued with the gradual rolling of the flattened inflatable by successive lifting and rotations of the partial folds by using the rigid plates defined previously. Three sets of lifting and rotation maneuvers, combined with the action of vertical gravity force, were applied to complete the folding sequence. Figure 6 illustrates the sequence of the last set of folding maneuvers and the inflatable in resultant final folded configuration.

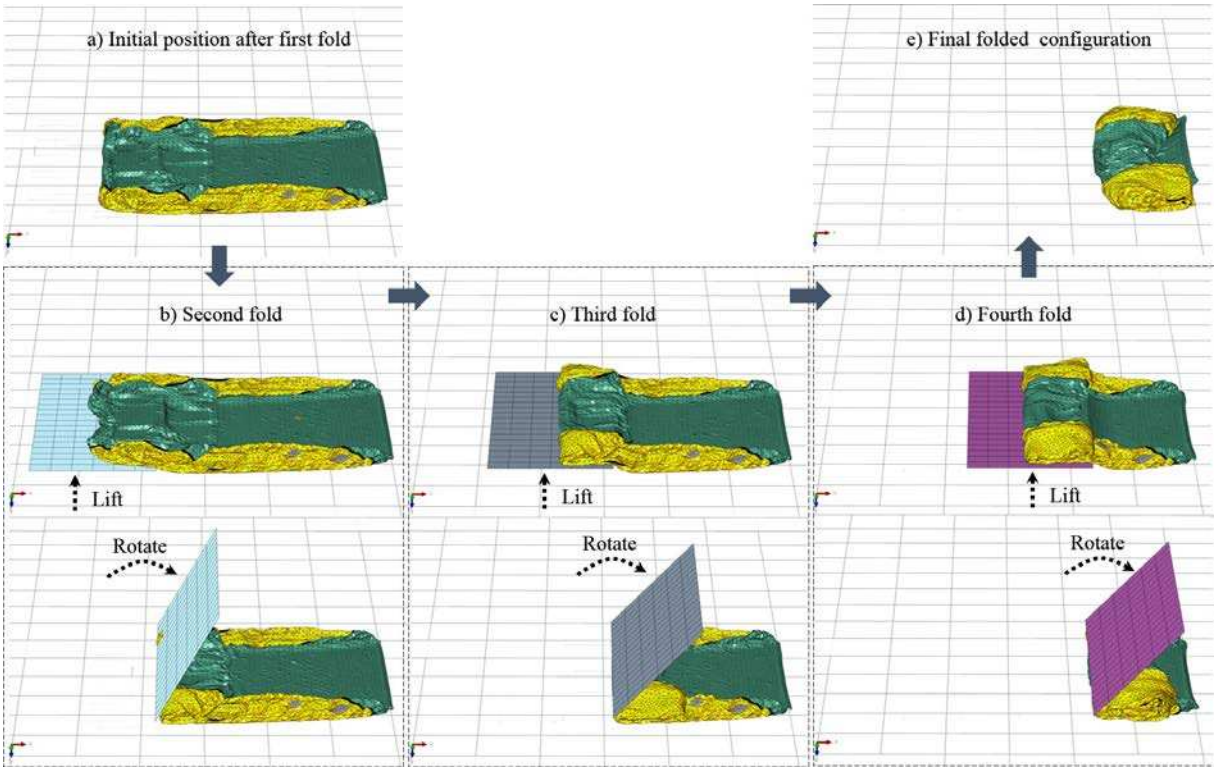

Figure 6: Simulation of folding (Part 2). Sequence of successive translation and rotation of auxiliary plates.

3.3 Simulation of placement of folded inflatable

The simulation of the placement process consisted of a combination of a rigid body rotations and translations of the folded inflatable to approach it and place it within the storage area of the tunnel segment. Once the folded inflatable was approached to the storage area, it was connected to the tunnel along a predefined horizontal line located inside the storage area (Figure 7(a)). As in the experimental work, the connecting line provided alignment to the inflatable during the initial deployment and maintained it connected to the tunnel during the inflation process. The placement continued with a horizontal translation produced by the action of a horizontal gravity force as shown in Figure 7(b). Once the folded inflatable was positioned within the storage area, a vertical rigid plane representative of the actual enclosure was approached and connected to the tunnel to hold the folded inflatable within the storage volume.

The rigid plane not only simulates the enclosure but also maintains the folded inflatable plug within the storage area during the implementation of the numerical relaxation process. The main purpose of implementing the numerical relaxation process into the simulation is to restore distorted elements back to their original condition before executing the deployment and inflation simulation. Abaqus/Explicit restores distorted elements through mapping of the coordinates of nodes from an initial configuration (in this case the folded configuration) to a

reference configuration defined by a metric file created for the inflatable under unconstrained conditions (Abaqus, 2011). The restoration is process was applied in conjunction with a vertical gravity force applied to the folded plug. The result of both effects defined the starting position for the simulation of deployment and inflation. The numerical relaxation process was also kept active during the deployment simulation to stabilize the simulation and to minimize excessive distortions on the membrane when the inflatable is fully positioned and confined by the tunnel inner perimeter at the end of the inflation.

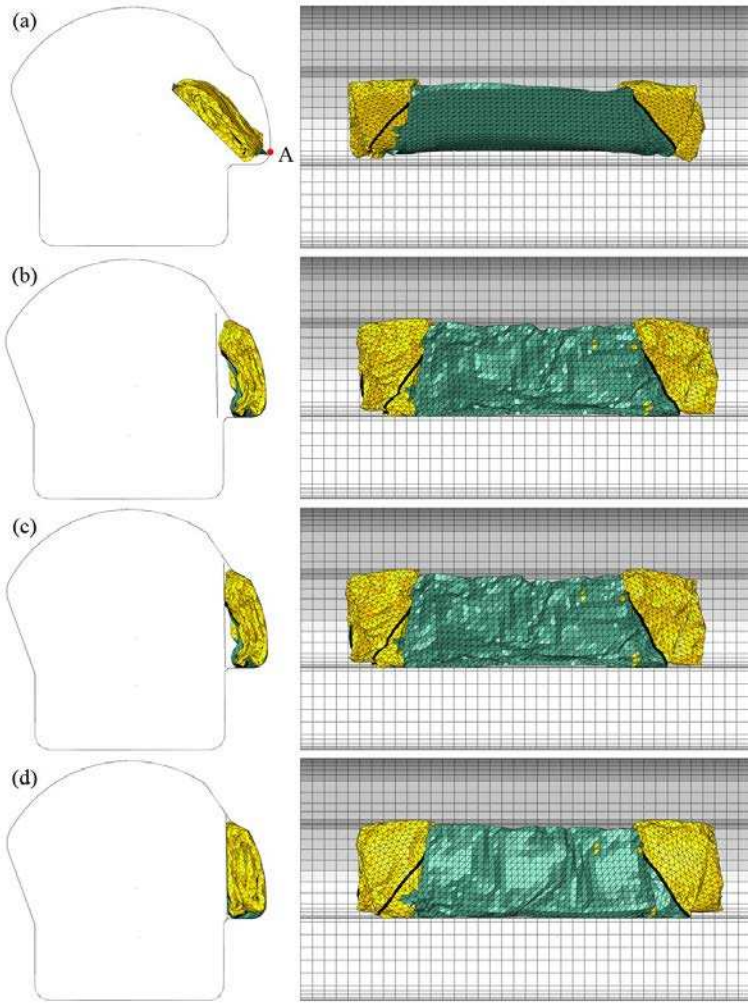

Figure 7: Placement of folded inflatable in tunnel section. (a) Approach and connection of the storage area; (b) Application of horizontal gravity force and approach of vertical cover; (c) Closure of storage area; (d) Final position after completion of the placement.

3.4 Simulation of inflation

The Uniform Pressure Method (UPM) proposed by Wang and Nefske (1988) and implemented in Abaqus/Explicit (Abaqus, 2011) was used to simulate the inflation process. For more than two decades, the UPM has been extensively implemented in simulations of airbags used by the automobile industry and demonstrated to predict good results (Buijk and Florie, 1991; Wang, 1995; Kamiji and Kawamura, 2001; Ha et al. 2004; Lee et al. 2009; Potula et al. 2012; Graczykowski, 2013). The UPM method is relatively simple to implement, computationally efficient and adequate for modeling relatively low-speed inflation since the

inertia of the inflation gas can be neglected. The capability of reproducing the inflation behavior at a relatively low computational cost and reasonable accuracy were two of the key factors that led to the adoption of the UPM as inflation method.

The UPM required the definition of surface-based cavities to model the fluid-structure interaction during the inflation process. This capability allowed to use standard elements to model the membrane of the inflatable and required a surface definition on the cavity boundary for coupling the deformation of the membrane and the pressure exerted by the inflation fluid (air at ambient temperature in this case). The UPM also required the definition of the fluid behavior, the fluid exchange to model the fluid flow and the definition of an inflator linked to one of the cavities (Abaqus, 2011). The UPM assumes that the pressure in the inflatable is spatially uniform during the inflation; it also assumes that there is no heat transfer (adiabatic process) and that the inflating gas behaves as an ideal gas with constant specific heats. A limitation of the UPM is the inability to simulate local fluid effects because the formulation does not involve the equations of fluid dynamics that describe the movement of fluid. However, this limitation was overcome by the implementation of a multi-chamber approach and the definition of fluid exchanges that extended the capability of the UPM. The implementation of these two additional approaches contributed to replicate better the inflation behavior observed in the full-scale experiments. The position of the internal chambers delimited by chamber walls placed inside the inflatable as well as the sequence of airflow distribution is illustrated in Figure 8.

The pre-simulation conditions for modeling a confined inflatable are similar to the conditions typically applied to simulations of automobile airbags. However, additional assumptions were made to define better some of the particularities of confined inflatables for sealing tunnel sections. These additional assumptions are based on the behavior observed during actual deployments of full-scale experimental prototypes reported by Barbero et al. (2013a) and Sosa et al. (2014a), including:

- Gravity force in the vertical direction is applied on the entire inflatable from the beginning to the end of the simulation.
- Air at an ambient temperature of 27°C (80°F) and standard ambient pressure of 100 kPa are assumed to exist during the inflation.
- Airflow rate of 42 m^3/min and a total analysis time of 200 seconds.
- Air transfer into and within the inflatable through an orifice with a discharge coefficient of 1.0.
- Airflow enters into the inflatable through only one of the inflation fittings.
- Walls of internal chambers directed the airflow inside the inflatable. The walls do not contribute to the mass or stiffness of the main membrane structure. The longitudinal and transverse walls that delimit the internal chambers are permeable to the inflation fluid, except when a specific fluid exchange is defined.
- The equivalent external membrane is assumed to be impermeable.

The folded inflatable placed in the storage area as illustrated in Figure 7(d) was used as starting point for initial deployment and inflation simulation. In this configuration, the folded plug sits on the base of the storage area under the effect of its own weight. A virtual vertical gate holds it up until the deployment sequence is activated. The folded plug is connected to the tunnel section at line A as shown in Figure 7(a), and the nodes of this line are cannot translate but are allowed to rotate in any direction. This boundary condition represents the ties that fasten and restrain the inflatable to the tunnel section and are assumed to be unbreakable

during the initial deployment and inflation simulation.

An important consideration is that in the modeling of folded membranes, distortions of the mesh and elements are introduced inevitably during the folding process. These distortions in the folded mesh may lead to initial stresses that can affect the final shape of the deployed inflatable structure by creating fictitious wrinkles and bogus stress concentrations that do not exist in the real membrane. In order to minimize this effect, the folded plug illustrated in Figure 7(d) was used as initial configuration and the mesh illustrated in Figure 4(b) was defined as a reference (or initial metric) to specify the unfolded stress-free configuration of the inflatable. Under this procedure, given that the reference configuration is specified for all the membrane elements, any initial stress conditions specified for the same element are neglected, and therefore no initial stresses were included in the membrane of the folded inflatable (Abaqus, 2011).

A friction coefficient 0.19 was used between the inflatable and the inner surface of the tunnel. A self-friction coefficient of 0.21 was used for the fabric-to-fabric friction. These two friction coefficients define how the surface of the membrane interacts with itself and the tunnel surface as the deployment and inflation develop during the simulation (Sosa et al. 2014b; Peil et al. 2012). The hard contact option was selected to be the contact method between parts (Abaqus, 2011).

Three representative inflation simulations are summarized in Table 1. In simulation S1, the folded inflatable did not include tie-downs to control the membrane release, and the airflow was not directed once it entered into the inflatable. That is, when the airflow entered through the inflation fitting, the air filled up all the internal chambers of the inflatable evenly and simultaneously as shown in Figure 8(b). In simulation S2, the folded inflatable included tie-downs installed during the folding process. Also, as in simulation S1, the airflow was not directed once it entered into the inflatable. Simulation S3 included tie-downs to control the membrane release. It also included specific fluid exchange designed to guide the airflow once it entered into the plug. In this case, the airflow fills up the first longitudinal half of the inflatable (longitudinal Chamber 1) immediately after entering the chamber through the inflation fitting. After a partial inflation of longitudinal Chamber 1, the second half of the inflatable (longitudinal Chamber 2) receives airflow from longitudinal Chamber 1 until the inflation is completed. The sequence of fluid exchange for simulation S3 is shown in Figure 8(c).

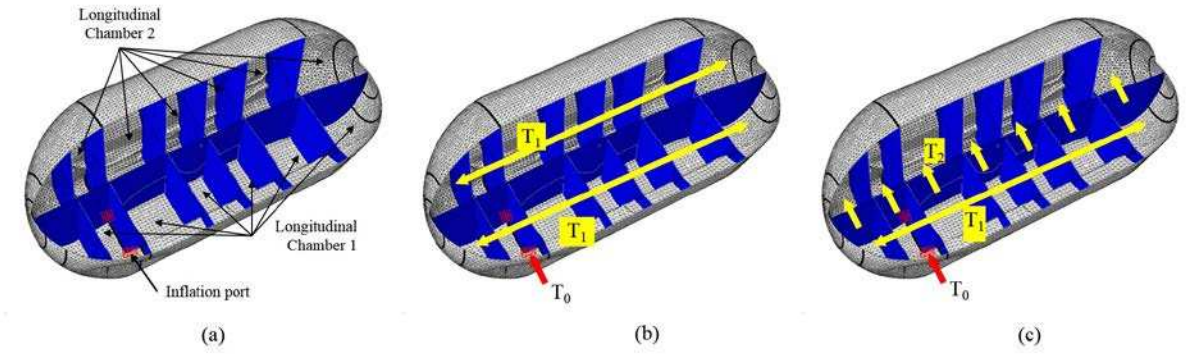

Figure 8: (a) Internal chamber distribution. (b) Inflation scheme 1, at T_0, the airflow enters into the inflatable, at T_1 the airflow filled both longitudinal chambers 1 and 2 simultaneously. (c) Inflation scheme 2, at T_0, the airflow enters into the inflatable, at T_1, the airflow filled longitudinal chamber 1 and then, at T_2, the airflow starts the inflation of longitudinal chamber 2.

Simulation	Tie-downs for sequential membrane release	Airflow directed within longitudinal chambers
S1	No	No
S2	Yes	No
S3	Yes	Yes

Table 1: Inflation simulation cases.

3.5 Results

As seen in the experiments, the initial deployment starts upon removal of the vertical gate that holds the inflatable within the storage area as shown in Figure 7(d). Then, the action of a vertical gravity force induces first, a slump of the membrane material, and then, unroll of the inflatable, which falls by its self-weight out of the container and rolls out towards the tunnel floor. This initial step takes the around 2 seconds as illustrated in the sequence of Figure 9. This initial movement was common for all three deployment models (S1 to S3). Immediately upon completion of the initial unrolling, the inflator was activated initiating the inflation process. Figure 9 illustrates the inflation process as a sequence of images captured from simulation models S1, S2, and S3 compared to experimental results.

In Figure 9, the effects of internally directing the internal airflow within the three models are seen between the 50^{th} second and 95^{th} second of the inflation sequence. The airflow in models S1 and S2 was not directed, so the inflation pressure was uniformly applied to both longitudinal chambers according to the sequence illustrated in Figure 8(b). In model S3, the inflation pressure was applied first to one-half of the inflatable (the one on the container side), and then to the second half (the one opposite side of the container) as shown in Figure 8(c). The delay in transferring the airflow changed the profile of the inflation sequence as seen in the images captured by the three models during the 50^{th} and 95^{th} seconds.

The effects of restraining the membrane during the inflation are seen between the 95^{th} second and the 140^{th} seconds of the inflation. In model S1, the membrane was not restrained during the folding process. In this case, once the inflatable has finished positioning at the bottom of the tunnel section, the inflation pressure pushed the membrane up until reaching the ceiling of the tunnel. In models S2 and S3, the tie-downs installed during the folding process held the membrane until the inflation pressure broke them around the 155^{th} second of the inflation and released the stored membrane that covered the upper portion of the tunnel cross-section.

Looking at all the simulation results in comparison with the experimental results of Figure 9, model S2 appears to follow more closely the inflation pattern observed in the experimental evaluations. This result suggests that the inflation scheme 1 illustrated in Figure 8(b) in combination with the tie-downs temporarily holding the membrane could reproduce more accurately the inflation sequence. However, additional parametric evaluations along with further comparisons with experimental inflations would be necessary to confirm this result.

In Figure 9 also, it is seen that as the inflation reached the 200^{th} second, all simulation models reached an apparent similar final shape at the end of the inflation. Additional post-processing and further analysis of the simulation results allowed a better understanding of the dynamics of the inflation process as well as an assessment of the levels of local conformity and global contact corresponding to each model.

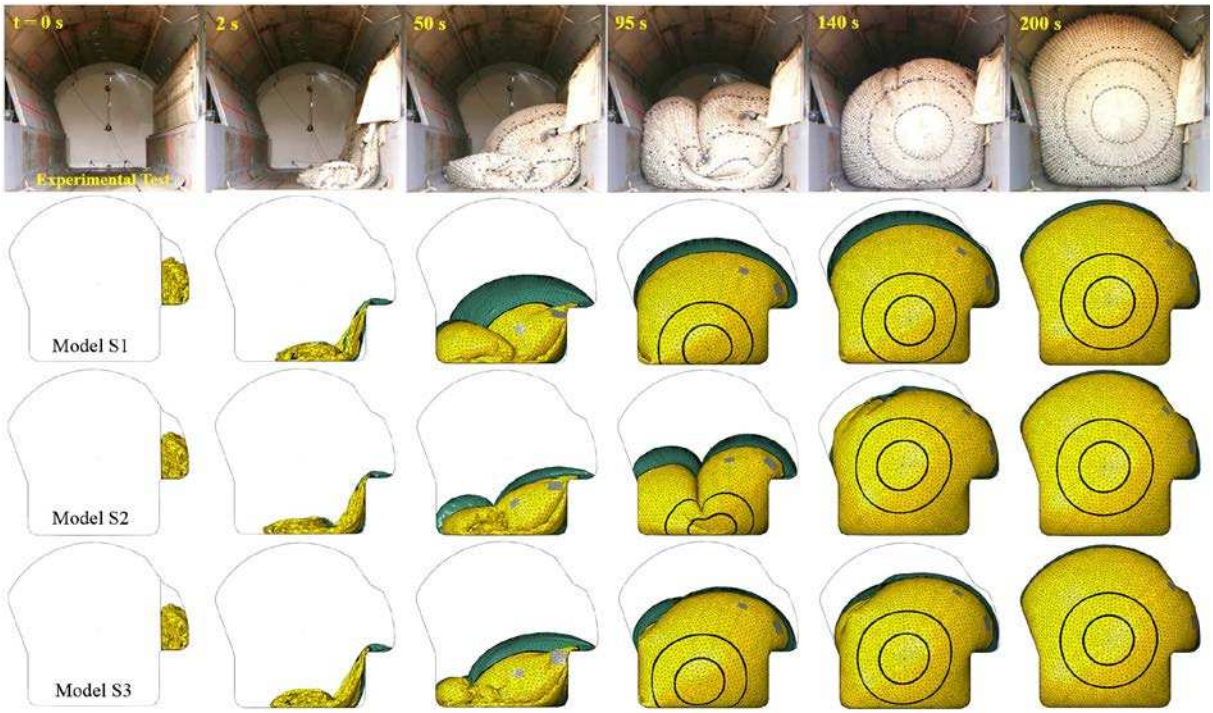

Figure 9: Comparison of experimental (Sosa et al. 2014a) and simulation results.

Figure 10 shows transversal and longitudinal cross-sections of the inflatable captured during the inflation process. Figure 10(a) shows transversal and longitudinal cross-sections corresponding to simulation S1 and Figure 10(b) shows transversal and longitudinal cross-sections corresponding to simulation S3. The cross sections of simulations S1 and S3 illustrate some characteristics of the inflation sequence that are useful to understand the dynamics of the inflation process. For example, the effect of guiding the airflow with the chambers of the inflatable is illustrated in the transversal cross-sections of Figure 10(a), Steps 4-5, where the internal chambers of model S1 started filling at the end of the initial unrolling. On the other side, the transversal cross-sections of model S3 illustrated in Figure 10(b), Steps 1-2, show that only the longitudinal chamber located on the container side of the tunnel is initially receiving airflow while the rest of the membrane remained deflated until the fluid exchange is activated in Step 3.

Another feature seen in the cross-sections is the membrane distribution at the different stages of the inflation. Following to the initial unroll and due to the gravity effect, practically all the membrane material is initially accumulated on the tunnel floor. As the inflation progresses, the membrane material moves from the storage side to the opposite side of the tunnel. This type of behavior is due to the folding pattern selected for the inflatable. Folding by rolling or by creating flat rolls favors a more uniform distribution of the membrane material. The inflation pressure also contributes to stretch longitudinal and transverse wrinkles by gradually dispersing the membrane material accumulated on the tunnel floor as seen in the longitudinal cross-sections of Figure 10(a) and 10(b). Note that in the images of simulation S1 shown in Figure 10(a) the walls of the internal chambers are displayed, but they do not contribute to the mass or stiffness of the inflatable.

A third feature observed in the transverse cross sections is the effect of having membrane material held by tie-downs during the inflation process. In model S1 the membrane of the cylindrical portion did not include tie-downs, and the membrane material is driven by the inflation pressure towards the tunnel ceiling. On the other hand, model S3 showed a better

material distribution and a better final coverage when the membrane was temporarily held and later released to cover the upper portion of the tunnel section better. The holding and release of the membrane are illustrated in the transversal and longitudinal cross-sections of Figure 10(b), Steps 3 to 5, where the inflation progressed until the tie-downs broke and released the membrane material reserved between the tie-downs. Since the pressure generated by the airflow continued being applied, it contributed to lifting the recently released membrane until it reaches the tunnel ceiling. As in the experimental work, the inclusion of tie-downs for temporarily holding off the membrane fulfilled two purposes during the inflation process: a) reserve membrane material for coverage of selected zones, in this case the upper portion of the tunnel section, and, b) reduce the formation of longitudinal wrinkles in the lower areas of the tunnel at the end of the inflation. The result of implementing this technique is an enhanced local conformity revealed by no gaps in the contact perimeter, which translates into an increased sealing capacity of the inflatable. All these observations are also consistent with the observations made during the full-scale experimental work (Barbero et al. 2013a and Sosa et al. 2014a).

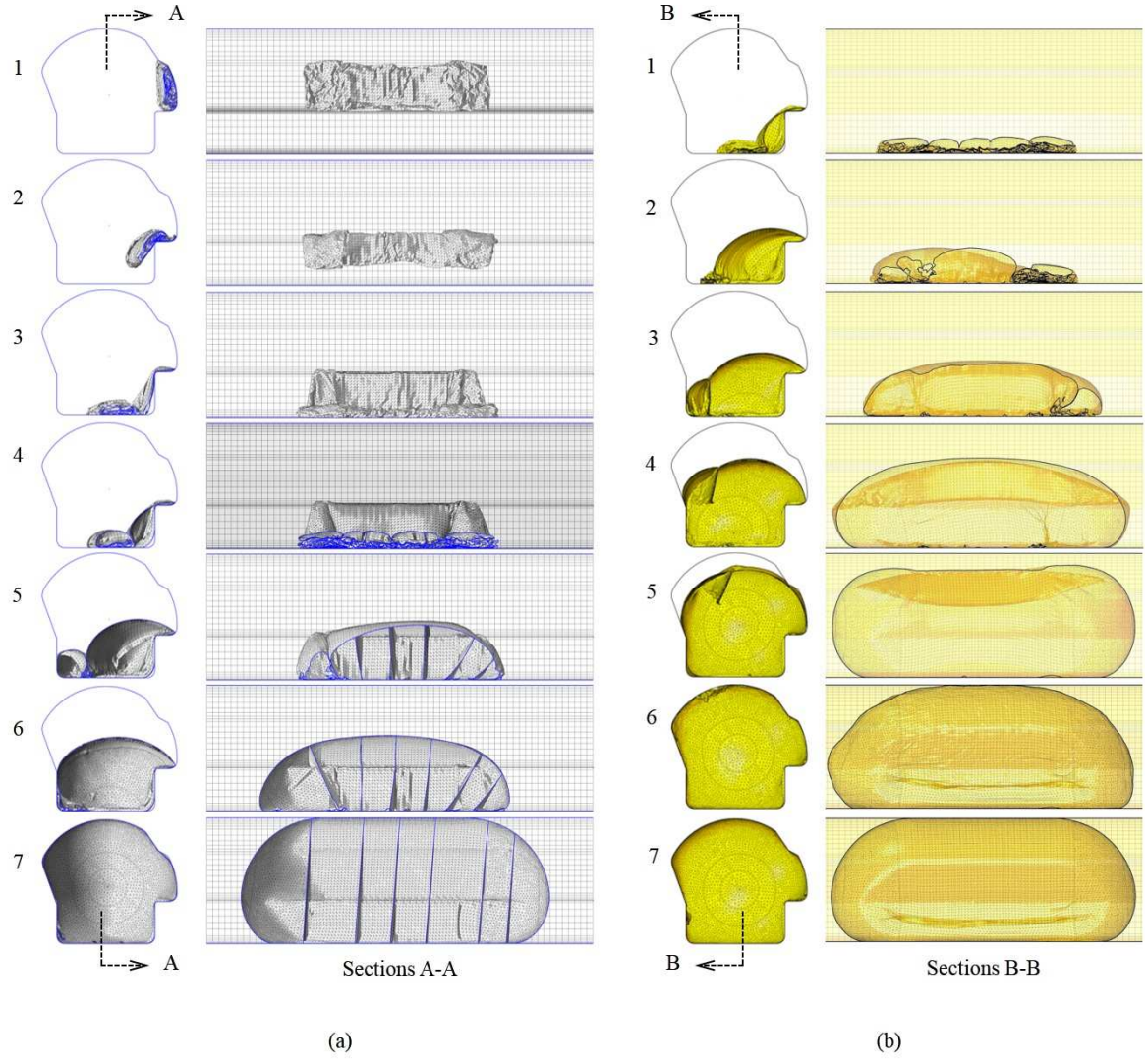

Figure 10: Transversal and longitudinal cross sections. (a) Model S1; (b) Model S3 (walls of internal chambers removed for clarity).

Figure 11 illustrates the level of local conformity obtained from simulation results in comparison with experimental results. The most critical areas for local conformity are the corners and transitions along the contact perimeter. Simulation S1 showed at least three visible gaps originated by bridging of the membrane, while models S2 and S3 did not show large visible gaps other than those associated with the local FE mesh density at the corners or transitions, as illustrated in the close-up views of Figure 11.

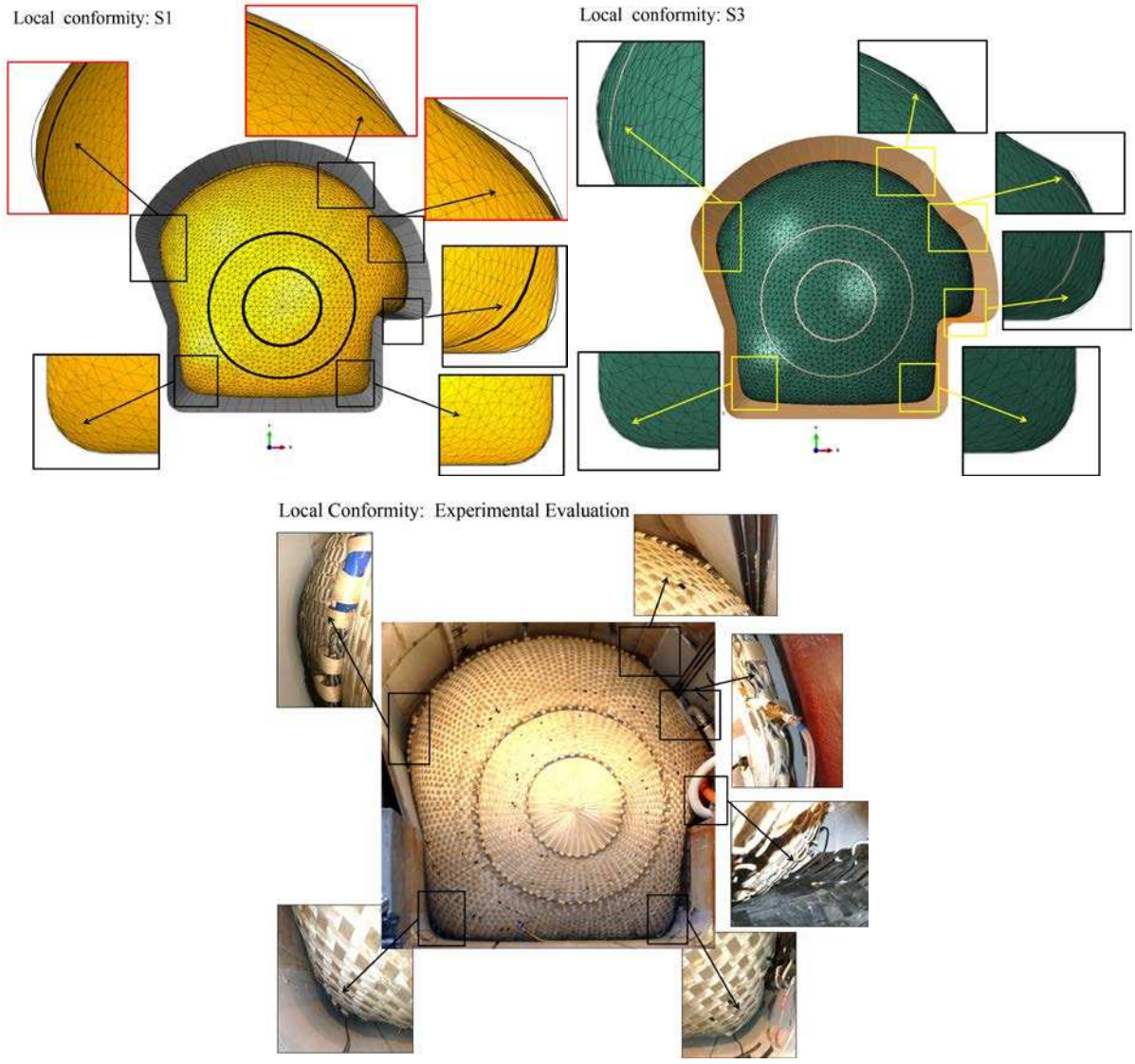

Figure 11: Evaluation of local conformity. Simulations S1 and S3 vs. experiments (Sosa et al. 2014a).

The level of global conformity of the inflatable to the tunnel section was evaluated by computing the contact area obtained for each deployment. An output obtained from Abaqus is the contact area between two objects, which in this case corresponded to the cylindrical portion of the inflatable and the tunnel inner perimeter. The inflatable plug was designed to have a cylindrical portion with a nominal contact area of 71.98 m². This contact area provides sufficient slippage resistance to hold the total external force originated by the flooding pressure applied to one of the hemispherical end caps. Looking at the longitudinal cross-sections of Figure 10 at the end of the inflation, it is clear that the final contact area is higher

than the design contact area, particularly at the tunnel floor level. The values of contact area at the end of the inflation summarized in Table 2 indicate that the contact area increased 25%, 32%, and 34%, for simulations S1, S2, and S3, respectively. The increase in the contact area is attributed to the confinement effect of the tunnel section in which part of the hemispherical end caps become part of the cylindrical portion of the plug, thus increasing the total contact area. However, this apparent increase in the final contact area should be taken with caution. Experimental observations indicated that when the inflatable plug is fully pressurized in preparation for flooding simulations, the two hemispherical end caps tended to regain their original hemispherical shape, and therefore reducing the apparent increase of contact area (Barbero et al. 2013a and Sosa et al. 2014a).

Simulation results show that the models can be used to evaluate the conformity, or fitness, of the inflatable to the tunnel geometry. The lack of conformity reveals itself in the form of bridging of the membrane at geometrical transitions such as sharp corners and around obstructions such as pipes or other obstacles to which the inflatable has to adapt to seal the tunnel. Experiments have shown that the lack of global and local conformity directly affects the leakage rate; that is, the flow rate that the plug is incapable of stopping because of the presence of gaps that reduced the sealing effectiveness of the inflatable.

Simulation Case	S1	S2	S3
Unconfined inflation, cylinder contact area (m^2)	71.98	71.98	71.98
Confined inflation, simulation contact area (m^2)	90.17	95.27	96.27
Contact enhancement (%)	+25%	+32%	+34%
Bridging spots (gaps in contact)	3	0	0

Table 2: Summary of contact area computed after completion of inflation.

4 CONCLUSIONS

This study presented an overview of the transition from experimental work to simulation work for the development and implementation of large-scale confined inflatable structures for sealing of tunnel sections. Previous experimental work was used as a reference for the creation of finite element models of the different stages of the experimental evaluations. Procedures and main features of the finite element models that reproduced the process of folding, placement, deployment of an inflatable structure were presented.

Overall, simulation results showed that the implementation of a modeling strategy that includes the application of geometric transformations for folding and positioning of the inflatable, as well as the implementation of the Uniform Pressure Method in combination with retardation devices or tie-downs, provided a reasonably accurate predicting tool. Simulation models displayed a good level of correlation with experimental results, particularly in reproducing the overall deployment dynamics consisting of the initial unrolling of the inflatable structure followed by full inflation within the tunnel section.

Simulation results also showed how a controlled release of membrane material during the inflation can lead to improved levels of local conformity and enhanced contact area between the surface of the inflatable and the tunnel inner surface. Considering that the actual contact area is not easily measurable in full-scale experiments, the simulation results can provide a good estimation of the actual contact area at the end of the initial inflation. Results also showed that the models can predict the global and local levels of conformity of the inflatable to the tunnel geometry by revealing gaps in the contact perimeter. Lack of local conformity

shows up in the form of bridging of the membrane material and the tunnel perimeter, particularly at corners, geometric transitions and around obstructions to which the membrane of the inflatable has to adapt to seal the tunnel perimeter.

The different features and assumptions used to create the FE simulation models will allow to carry out further analyses and parametric studies. The FE models developed under this work will allow performing assessments of the influence of changes in the shape of the confining tunnel perimeter, alternative folding sequences, alternative ways to guide the air flow within the inflatable plug and the influence of using different airflow rates during the inflation process. The assessment of variations of all these factors at experimental level can be very costly, so the availability of a validated simulation models contributes to minimizing the need for experimental evaluations.

5 REFERENCES

Abaqus User's Manual, *Documentation Collection Version 6.11*, Dassault Systémes Simulia Corp., Providence, RI, 2012.

Barbero, E.J., Sosa, E.M., and Thompson, G.J. Testing of Full-Scale Confined Inflatable for the Protection of Tunnels. *Proceedings of the VI International Conference on Textile Composites and Inflatable Structures, Structural Membranes 2013*, Munich, Germany, October 9-11, 2013a.

Barbero, E.J., Sosa, E.M., Martinez, X., Gutierrez, J.M., Reliability Design Methodology for Confined High-Pressure Inflatable Structures. *Engineering Structures*, 51:1-9, 2013b.

Barrie, A. Going Underground: Homeland Security Works on Tool to Prevent Tunnel Disasters, 2008. http://www.foxnews.com/story/0,2933,417461,00.html.

Buijk, A.J., and Florie, C.J.L., Inflation of folded driver and passenger airbags. *Proceedings of the MSC World Users Conference*, Paper 91-04-B, Los Angeles, California, March, 1991.

Fountain, H. Holding Back Floodwaters with a Balloon. *The New York Times/Science Supplement*, 2012. http://www.nytimes.com/2012/11/20/science/creating-a-balloonlike-plug-to-hold-back-floodwaters.html.

Graczykowski, C., Theoretical models and numerical methods for adaptive inflatable structures. *Proceedings of the Fourteenth International Conference on Civil, Structural and Environmental Engineering Computing*, Stirlingshire, Scotland, 2013.

Ha, W.P., Park S.J., and Spit H.H., Advanced curtain airbag modeling using the uniform pressure approach combined with a gas flow analysis. *SAE*, 01-1632, 2004.

Kamiji, K., Kawamura, N., Study of airbag interference with out of position occupant by the computer simulation. *Proceedings of the 17th International Technical Conference on the Enhanced Safety of Vehicles (ESV)*, Paper #374, Amsterdam, Netherlands, June 4-7, 2001.

Kuraray Co., Homeland Security: A Big Plug for Vectran, 2012. http://www.kuraray.us.com/kuraray-vectran-material-used-in-subway-plug

Lee, J.K., Ha, W.P., Lee, J.H., Chae, D.B., and Kim, J.H., Validation methodology on airbag deployment process of driver side airbag. *Proceedings of the 21th Enhanced Safety of Vehicles (ESV) Conference*, Paper No. 09-0363, Stuttgart, Germany, June 15–18, 2009.

Lindstrand Technologies, Inflatable Tunnel Plugs, 2010. http://www.lindstrandtech.com/innovation-centre-main/innovation-centre/inflatable-tunnel-plugs.

Martinez, X., Davalos, J., Barbero, E.J., Sosa, E.M., Huebsch. W., Means, K., Banta, L., and Thompson, G.J., Inflatable Plug for Threat Mitigation in Transportation Tunnels.

Proceedings of the Society for the Advancement of Material and Process Engineering Conference, Baltimore, MD, May 21-24, 2012.

Peil, K.L., Barbero, E.J., and Sosa, E.M., Experimental Evaluation of Shear Strength of Woven Webbings. *Proceedings of the Society for the Advancement of Material and Process Engineering Conference*, Baltimore, MD, May 21-24, 2012.

Potula, S.R., Solankia, K.N., Oglesby, D.L., Tschopp, M.A., Bhatia, M.A., Investigating occupant safety through simulating the interaction between side curtain airbag deployment and an out-of-position occupant. *Accident Analysis and Prevention*, 49:392– 403, 2012.

Sosa, E.M., Thompson, G.J., and Barbero E.J., Testing of full-scale inflatable plug for flood mitigation in tunnels. *Transportation Research Record: Journal of the Transportation Research Board*, 2407, 2:59-67, 2014a.

Sosa, E.M., Thompson, G.J., Barbero, E.J., Ghosh, S., and Peil, K.L., Friction characteristics of confined inflatable structures. *Friction*, 2(4):365–390, 2014b.

Sosa, E.M., Barbero, E.J., and Thompson, G.J., Design and Testing Inflatable Plugs for Flood Containment in Tunnels. *Rev. Int. de Desastres Naturales, Accidentes e Infraestructura Civil*, 14(1-2), 39-57, 2014c.
http://academic.uprm.edu/laccei/index.php/RIDNAIC/issue/view/39.

Wang, J.T., An analytical model for an airbag with a hybrid inflator. *General Motors Research & Development Center, Crashworthiness and Occupant Protection in Transportation Systems, ASME*, AMD-210/BED-30, 1995.

Wang, J.T., and Nefske, D.J., A new CAL3D airbag inflation model. *SAE Technical Paper Series 880654. International Congress and Exposition*, Detroit, MI, February 29 – March 4, 1988.